THE CATHOLIC UNIVERSITY OF AMERICA
DEPARTMENT OF ELECTRICAL ENGINEERING

DESIGN OF AN ADAPTIVE CONTROLLER FOR A TELEROBOT MANIPULATOR

Charles C. Nguyen
Principal Investigator and Associate Professor
and
Zhen-Lei Zhou
Graduate Research Assistant

submitted to
Mr. Gary E. Mosier
Code 712.1
Goddard Space Flight Center (NASA)
Greenbelt, Maryland

August 1989

SUMMARY

In this report, we present the research results from the research grant entitle "Development of Advanced Control Schemes for Telerobot Manipulators," funded by the Goddard Space Flight Center, under the Grant Number NAG 5-1124 for the period between March 1, 1989 and August 31, 1989.

This report presents the design of a joint-space adaptive control scheme for controlling the slave arm motion of a dual-arm telerobot system developed at Goddard Space Flight Center (GSFC) *to study telerobotic operations in space. Each slave arm of the dual-arm system is a kinematically redundant manipulator with 7 degrees of freedom* (DOF). *Using the concept of model reference adaptive control* (MRAC) *and Lyapunov direct method we derive an adaptation algorithm which adjusts the PD controller gains of the control scheme. The development of the adaptive control scheme assumes that the slave arm motion is non-compliant and slowly-varying. The implementation of the derived control scheme does not need the computation of the manipulator dynamics, which makes the control scheme sufficiently fast for real-time applications. Computer simulation study performed for the 7-DOF slave arm shows that the developed control scheme can efficiently adapt to sudden change in payloads while tracking various test trajectories such as ramp or sinusoids with negligible position errors.*

1 INTRODUCTION

Telerobotics, a concept combined by two principles, *teleoperation* and *robotics* [1] has attracted tremendous research attention because it has potential applications in hazardous environments such as the future NASA space station, nuclear power plants, or undersea. Extravehicular activities such as assembly, maintenance or inspection in space, can be made less dangerous by cooperating astronauts and telerobots in a telerobotic operation. Depending on the complexity of the task to be performed, the astronaut can be either assisted or replaced by the telerobot. Teleoperations can be performed either in a *teleoperated control mode* or in a *autonomous control mode* [2]. In the teleoperated control mode, the astronaut remotely controls the motion of the slave arm of the telerobot using a master arm system. On the other hand, the slave arm performs its motion autonomously under the supervision of the astronaut, in the autonomous control mode. In any mode, to achieve a successful task, precise control of the slave arm motion should be ensured.

Goddard Space Flight Center (**GSFC**) is developing a Flight Telerobotic Servicer (**FTS**) to perform a variety of tasks on the NASA space station, which include assembly, inspection, servicing, and maintenance. To support the FTS development, a dual-arm telerobot system consisting mainly of a pair of 6-DOF mini-master controllers and a pair of 7-DOF slave arms has been built at GSFC to serve as a testbed for studying a variety of issues such as zero-g operation, dual-arm robot control, advanced control schemes, and hierarchical control etc. [3]. This report concerns with the motion control of the slave arm which is a kinematically redundant robot manipulator.

Control of redundant robot manipulators, defined as manipulators having more DOF than necessary to perform a specified tasks has been an active research area [4]-[7] because of its many advantages including the use of extra DOF to maneuver in a congested workspace and avoid collisions with obstacles. Most conventional control schemes such as *Computed Torque Technique* [8], are derived based on the dynamic modeling the robot manipulator. Since in addition to the massive computation requirement in evaluating dynamic models in real-time control, it is almost impossible to derive an accurate dynamic model for a robot manipulator, the above developed control schemes are generally not feasible. In an attempt to alleviate the problem of uncertainties in manipulator dynamics and payloads, considerable research effort has been focused on studying *Adaptive Control* [9]. Lyapunov method and MRAC were used to design adaptive controllers for trajectory control, which was proved to provide global stability [10]. The authors in [11] considered the design of robust adaptive controllers. Adaptive force control problem was investigated in [12] for a cutting problem. In [13] an adaptive force-position controller with self-tuning was designed in Cartesian space by using eigenvalue assignment method and minimization of a quadratic performance criterion. Research work in [14] resulted in the development of a decentralized adaptive control scheme based on independent joint control concept. A joint-space adaptive control scheme was developed in [15] to control the motion of a robotic end-effector with closed kinematic chain mechanism [16]. The problem of hybrid control of force and position was considered in [17]. Employing the Kalman filter, the authors in [18] proposed an approach to adaptive control of manipulators based on an identification scheme. Recently, MRAC and Lyapunov method were employed in [19] to design a joint-space adaptive control scheme for a telerobot manipulator.

The organization of this report is as follows. In the next section, we first describe the struc-

ture and operations of the GSFC telerobot testbed. Next a joint-space adaptive control scheme is developed using MRAC and Lyapunov method. We then present the computer simulation performed to study the performance of the developed adaptive control scheme which is implemented to control the motion of the 7 DOF slave arms, and evaluate the simulation results. Finally in the conclusion, we discuss the results of the report and outline some future research directions.

The following notations are used in this report:

- $\mathbf{M}^T$: transpose of the matrix M
- $\mathbf{0}_n$: (nxn) matrix whose elements are all zero
- $\mathbf{I}_n$: (nxn) identity matrix.

2 THE NASA TELEROBOT TESTBED

Figure 1 presents the dual-arm telerobot system recently developed at GSFC to serve as a testbed for investigating the feasibility of telerobotic operations in space. The system mainly consists of a pair of slave arms, each of which is a 7-DOF kinematically redundant robot manipulator, manufactured by Robotics Research Cooperation (**RRC**) and a pair of 6-DOF Kraft Mini-Master (**KMM**) hand controllers from Kraft Telerobotics, Inc. At this time, the RRC controllers have been modified by GSFC engineers to allow implementation of advanced control schemes, and to incorporate other advanced features such as high-speed parallel processing.

The operations of the telerobot system can be best explained using the block diagram given in Figure 2. The RRC slave arm system receives actual data of joint force and joint positions/velocities via force sensors and joint position/velocity sensors mounted on the slave arms. Joint forces that are transmitted to the KMM system for force reflection can be determined using the slave arm joint forces. In a teleoperated control mode, the human operator residing in an operator control station such as Space Shuttle, Space Station, or on ground, controls the motion of the slave arms via the mini-master controllers using familiar hand and arm movements while observing the slave arm motion and the task space from a cupola, a window or a TV monitor. The force/torque applied by the human operator produces 6 joint positions in the master arm system, which then are converted to 7 corresponding joint positions in the slave arm system through an appropriate coordinate transformation. The 7 joint positions of the slave arms will then serve as the desired variables to be supplied to a control system in the RRC system. Based on the difference between the desired joint variables and the actual joint variables of the slave arms, provided by feedback data, the controller then employs a control scheme to provide necessary control signals to the actuators of the slave arms so that it tracks the desired motion as closely as possible while maintaining a desired contact force on the task environment. In an autonomous control mode where the slave arms perform the task autonomously while the human operator plays only a supervisory role, the desired inputs to the slave arm control system can be generated by a *Path Planner.*

3 DESIGN OF THE ADAPTIVE CONTROLLER

Since the desired inputs to the slave arm control system are expressed as joint variables, as explained in previous section, a joint-space control scheme should be considered to avoid the time-consuming evaluation of the forward and inverse kinematics when a Cartesian-space control scheme is employed in real-time control. Also to effectively react to the nonlinearity of the manipulator dynamics, errors in dynamic modeling, and sudden change in payloads, adaptive controllers should be developed instead of fixed-gain controllers which work well only when the manipulator stays within the linearized operating region [10].

The following development of the adaptive control scheme focuses on controlling the motion of a single slave arm performing non-compliant motion, i.e. the slave arm moves freely in space without being in contact with the environment. In this case, pure position control scheme can be employed to control the motion of the slave arm, since contact force control is not needed. Hybrid position/force control scheme can be applied in the case of compliant motion [17]. Furthermore, we assume that the arm motion is slowly varying because rapid motion of the slave arms is considered to be dangerous during a telerobotic operation, especially in obstacle avoidance.

The dynamics of the 7-joint slave arm can modeled by the following nonlinear vector differential equation [19]:

$$\tau(t) = \mathbf{M}(\mathbf{q}, \dot{\mathbf{q}})\, \ddot{\mathbf{q}}(t) + \mathbf{N}(\mathbf{q}, \dot{\mathbf{q}})\, \dot{\mathbf{q}}(t) + \mathbf{G}(\mathbf{q}, \dot{\mathbf{q}})\, \mathbf{q}(t) \tag{1}$$

where $\mathbf{q}$(t) denotes (7x1) joint positions of the slave arm, τ(t), the (7x1) joint force vector, $\mathbf{M}(\mathbf{q}, \dot{\mathbf{q}})$, the slave arm mass matrix is a symmetric positive-definite matrix of order (7x7), $\mathbf{N}(\mathbf{q}, \dot{\mathbf{q}})$ and $\mathbf{G}(\mathbf{q}, \dot{\mathbf{q}})$ are (7x7) matrices whose elements are highly complex nonlinear functions of $\mathbf{q}$ and $\dot{\mathbf{q}}$. In the right-hand side of (1), if we neglect joint friction, the second term represents the centrifugal and Coriolis forces, and the third term the gravity forces.

An adaptive controller consisting of a Proportional (**P**) and a Derivative (**D**) terms is defined by

$$\tau(t) = \mathbf{K}_p(t)\, \mathbf{q}_e(t) + \mathbf{K}_d(t)\, \dot{\mathbf{q}}_e(t) \tag{2}$$

where

$$\mathbf{q}_e(t) = \mathbf{q}_d(t) - \mathbf{q}(t) \tag{3}$$

denotes the joint error vector between the actual joint vector $\mathbf{q}(t)$ and the desired joint vector $\mathbf{q}_d(t)$, $\mathbf{K}_p(t)$ and $\mathbf{K}_d(t)$ are the matrices of the proportional and derivative terms, respectively, of the adaptive controller.

Substituting (2) into (1) yields

$$\mathbf{M}\, \ddot{\mathbf{q}}_e + (\mathbf{N} + \mathbf{K}_d)\, \dot{\mathbf{q}}_e + (\mathbf{G} + \mathbf{K}_p)\, \mathbf{q}_e = \mathbf{M}\, \ddot{\mathbf{q}}_d + \mathbf{N}\, \dot{\mathbf{q}}_d + \mathbf{G}\, \mathbf{q}_d \tag{4}$$

where the dependent variables of the matrices and vectors were omitted for readability.

In order to transform (4) into a state space form, we proceed to define a (14x1) state vector $\mathbf{z}(t)$ such that

$$\mathbf{z}(t) = \left[\mathbf{q}_e^T(t) \quad \dot{\mathbf{q}}_e^T(t)\right]^T, \tag{5}$$

which rewrites (4) as

$$\dot{\mathbf{z}}(t) = \begin{bmatrix} \mathbf{0}_7 & \mathbf{0}_7 \\ -\mathbf{A}_1 & -\mathbf{A}_2 \end{bmatrix} \mathbf{z}(t) + \begin{bmatrix} \mathbf{0}_7 & \mathbf{0}_7 & \mathbf{0}_7 \\ \mathbf{A}_3 & \mathbf{A}_4 & \mathbf{I}_7 \end{bmatrix} \mathbf{u}(t) \tag{6}$$

where

$$\mathbf{A}_1 = \mathbf{M}^{-1}(\mathbf{G} + \mathbf{K}_p), \quad \mathbf{A}_2 = \mathbf{M}^{-1}(\mathbf{N} + \mathbf{K}_d), \tag{7}$$

and

$$\mathbf{A}_3 = \mathbf{M}^{-1}\,\mathbf{G}, \quad \mathbf{A}_4 = \mathbf{M}^{-1}\,\mathbf{N}, \tag{8}$$

and

$$\mathbf{u}(t) = \left[\mathbf{q}_d^T(t) \quad \dot{\mathbf{q}}_d^T(t) \quad \ddot{\mathbf{q}}_d^T(t)\right]^T. \tag{9}$$

In the framework of MRAC, Equation (6) represents the *adjustable system*. The desired performance of the slave arm motion can be specified by a *reference model* in terms of the tracking error vector $\mathbf{q}_e(t) = [q_{e1}(t)\ q_{e2}(t) \ldots q_{e7}(t)]^T$. Suppose the tracking errors $q_{ei}(t)$ for i=1,2,...,6, are decoupled from each other, and satisfy

$$\ddot{q}_{ei}(t) + 2\,\xi_i\,\omega_i\,\dot{q}_{ei}(t) + \omega_i^2\,q_{ei}(t) = 0 \tag{10}$$

for i=1,2,...,6, where ξ_i and ω_i denote the damping ratio and the natural frequency of q_{ei}, respectively. Then the dynamics of the reference model can be represented by

$$\dot{\mathbf{z}}_m(t) = \mathbf{D}\,\mathbf{z}_m(t) = \begin{bmatrix} \mathbf{0}_7 & \mathbf{I}_7 \\ -\mathbf{D}_1 & -\mathbf{D}_2 \end{bmatrix} \mathbf{z}_m(t), \tag{11}$$

where $\mathbf{D}_1$=diag(ω_i^2) and $\mathbf{D}_2$=diag($2\xi_i\omega_i$) are constant (7x7) diagonal matrices, and

$$\mathbf{z}_m(t) = \left[\mathbf{q}_m^T(t) \quad \dot{\mathbf{q}}_m^T(t)\right]^T \tag{12}$$

with

$$\mathbf{q}_m = (q_{e1}\ q_{e2}\ \cdots q_{e7})^T. \tag{13}$$

Solving (11), we obtain

$$\mathbf{z}_m(t) = \exp(\mathbf{D}t)\,\mathbf{z}_m(0). \tag{14}$$

We note from (14), that if $\mathbf{z}_m(0) = 0$, i.e. the initial values of the actual and reference joint vectors are identical, then $\mathbf{z}_m(t) = 0$.

Now if $\mathbf{e}(t)$, the adaptation error vector is defined as

$$\mathbf{e}(t) = \mathbf{z}_m(t) - \mathbf{z}(t), \tag{15}$$

then from (6) and (11), we obtain an error system described by

$$\begin{aligned} \dot{\mathbf{e}}(t) \;=\; & \begin{bmatrix} \mathbf{0}_7 & \mathbf{I}_7 \\ -\mathbf{D}_1 & -\mathbf{D}_2 \end{bmatrix} \mathbf{e}(t) + \begin{bmatrix} \mathbf{0}_7 & \mathbf{0}_7 \\ \mathbf{A}_1 - \mathbf{D}_1 & \mathbf{A}_2 - \mathbf{D}_2 \end{bmatrix} \mathbf{z}(t) \\ & + \begin{bmatrix} \mathbf{0}_7 & \mathbf{0}_7 & \mathbf{0}_7 \\ -\mathbf{A}_3 & -\mathbf{A}_4 & -\mathbf{I}_7 \end{bmatrix} \mathbf{u}(t). \end{aligned} \tag{16}$$

We proceed to select a Lyapunov function candidate $v(t)$ such that

$$\begin{aligned} v(t) \;=\; & \mathbf{e}^T\mathbf{P}\mathbf{e} + tr\left[(\mathbf{A}_1 - \mathbf{D}_1)^T\boldsymbol{\Pi}_1(\mathbf{A}_1 - \mathbf{D}_1)\right] \\ & + tr\left[(\mathbf{A}_2 - \mathbf{D}_2)^T\boldsymbol{\Pi}_2(\mathbf{A}_2 - \mathbf{D}_2)\right] \\ & + tr[\mathbf{A}_3^T\boldsymbol{\Pi}_3\mathbf{A}_3] + tr[\mathbf{A}_4^T\boldsymbol{\Pi}_4\mathbf{A}_4], \end{aligned} \tag{17}$$

where $tr[\mathbf{M}]$ is the trace of matrix $\mathbf{M}$, $\mathbf{P}$ and $\boldsymbol{\Pi}_i$ for i=1,2,...,4, are positive definite matrices to be determined later.

Taking the time derivative of (17) and simplifying the resulting expression, we obtain

$$\begin{aligned}\dot{v}(t) &= \mathbf{e}^T(\mathbf{PD}+\mathbf{D}^T\mathbf{P})\mathbf{e} \\ &\quad +2tr\left[(\mathbf{A}_1-\mathbf{D}_1)^T(\boldsymbol{\Omega}\mathbf{q}_e^T+\boldsymbol{\Pi}_1\dot{\mathbf{A}}_1)\right] \\ &\quad +2tr\left[(\mathbf{A}_2-\mathbf{D}_2)^T(\boldsymbol{\Omega}\dot{\mathbf{q}}_e^T+\boldsymbol{\Pi}_2\dot{\mathbf{A}}_2)\right] \\ &\quad -2tr\left[\mathbf{A}_3{}^T(\boldsymbol{\Omega}\mathbf{q}_d^T-\boldsymbol{\Pi}_3\dot{\mathbf{A}}_3)\right] \\ &\quad -2tr\left[\mathbf{A}_4{}^T(\boldsymbol{\Omega}\dot{\mathbf{q}}_d^T-\boldsymbol{\Pi}_4\dot{\mathbf{A}}_4)\right] \end{aligned} \tag{18}$$

where

$$\boldsymbol{\Omega}=[\mathbf{P}_2\ \ \mathbf{P}_3]\mathbf{z}(t)=-\mathbf{P}_2\mathbf{q}_e-\mathbf{P}_3\dot{\mathbf{q}}_e \tag{19}$$

and $\mathbf{P}$ is given by

$$\mathbf{P}=\begin{bmatrix}\mathbf{P}_1 & \mathbf{P}_2\\ \mathbf{P}_2 & \mathbf{P}_3\end{bmatrix} \tag{20}$$

and it is noted that $\mathbf{e}(t)=-z(t)$ since $\mathbf{z}_m(t)=0$.

In (10) ξ_i and ω_i can be selected so that $\mathbf{D}$ is a matrix having stable eigenvalues, which is also called a *Hurwitz* matrix [20]. Therefore according to *Lyapunov theorem*, for any given positive-definite symmetric matrix $\mathbf{Q}$, there exists a positive definite symmetric matrix $\mathbf{P}$ that satisfies the Lyapunov equation

$$\mathbf{PD}+\mathbf{D}^T\mathbf{P}=-\mathbf{Q}. \tag{21}$$

Now in (18), if we set

$$\boldsymbol{\Omega}\mathbf{q}_e^T+\boldsymbol{\Pi}_1\dot{\mathbf{A}}_1=\boldsymbol{\Omega}\dot{\mathbf{q}}_e^T+\boldsymbol{\Pi}_2\dot{\mathbf{A}}_2=0 \tag{22}$$

and

$$\boldsymbol{\Omega}\mathbf{q}_d^T-\boldsymbol{\Pi}_3\dot{\mathbf{A}}_3=\boldsymbol{\Omega}\dot{\mathbf{q}}_d^T-\boldsymbol{\Pi}_4\dot{\mathbf{A}}_4=0, \tag{23}$$

then (18) becomes

$$\dot{v}(t)=-\mathbf{e}^T\mathbf{Qe} \tag{24}$$

which is a negative definite function of $\mathbf{e}(t)$. Furthermore, from (22)-(23), we obtain

$$\dot{\mathbf{A}}_1=-\boldsymbol{\Pi}_1^{-1}\boldsymbol{\Omega}\mathbf{q}_e^T;\ \ \dot{\mathbf{A}}_2=-\boldsymbol{\Pi}_2^{-1}\boldsymbol{\Omega}\dot{\mathbf{q}}_e^T, \tag{25}$$

and

$$\dot{\mathbf{A}}_3=\boldsymbol{\Pi}_3^{-1}\boldsymbol{\Omega}\mathbf{q}_e^T;\ \ \dot{\mathbf{A}}_4=\boldsymbol{\Pi}_4^{-1}\boldsymbol{\Omega}\dot{\mathbf{q}}_d^T. \tag{26}$$

We already showed that $\mathbf{P}$ is a positive definite matrix. Now if we could show that $\boldsymbol{\Pi}_i$ for i=1,2,...,4, are also positive definite matrices, then the error system described in (16) is asymptotically stable, i.e., $\mathbf{e}(t)\rightarrow 0$, or $\mathbf{z}(t)\rightarrow\mathbf{z}_m$ as $t\rightarrow\infty$.

As mentioned earlier, since we assume that the slave arm performs slowly varying motion, $\mathbf{M}$, $\mathbf{N}$ and $\mathbf{G}$ are *slowly time-varying matrices* which can be considered as *nearly constant matrices.* Consequently from (7) and (8) we obtain

$$\dot{\mathbf{A}}_1\simeq\mathbf{M}^{-1}\dot{\mathbf{K}}_p;\ \ \dot{\mathbf{A}}_2\simeq\mathbf{M}^{-1}\dot{\mathbf{K}}_d \tag{27}$$

and

$$\dot{\mathbf{A}}_3 \simeq 0; \;\; \dot{\mathbf{A}}_4 \simeq 0. \tag{28}$$

Next substitution of (27)-(28) into (25)-(26) yields

$$\mathbf{M}^{-1}\dot{\mathbf{K}}_p = -\boldsymbol{\Pi}_1^{-1}\boldsymbol{\Omega}\mathbf{q}_e^T; \;\; \mathbf{M}^{-1}\dot{\mathbf{K}}_d = -\boldsymbol{\Pi}_2^{-1}\boldsymbol{\Omega}\dot{\mathbf{q}}_e^T, \tag{29}$$

and

$$0 \simeq \boldsymbol{\Pi}_3^{-1}\boldsymbol{\Omega}\mathbf{q}_d^T; \;\; 0 \simeq \boldsymbol{\Pi}_4^{-1}\boldsymbol{\Omega}\dot{\mathbf{q}}_d^T. \tag{30}$$

Now in (29), letting

$$\boldsymbol{\Pi}_1 = -\frac{1}{\alpha_1}\mathbf{M}; \;\; \boldsymbol{\Pi}_2 = -\frac{1}{\alpha_2}\mathbf{M}, \tag{31}$$

where α_1 and α_2 are arbitrary positive scalars, and solving for $\dot{\mathbf{K}}_p$ and $\dot{\mathbf{K}}_d$, we obtain

$$\dot{\mathbf{K}}_p = \alpha_1\boldsymbol{\Omega}\mathbf{q}_e^T, \tag{32}$$

and

$$\dot{\mathbf{K}}_d = \alpha_2\boldsymbol{\Omega}\dot{\mathbf{q}}_e^T. \tag{33}$$

In (31), we note that $\boldsymbol{\Pi}_1$ and $\boldsymbol{\Pi}_2$ are positive definite matrices that can be considered as nearly constant because the slave arm mass matrix $\mathbf{M}$ is positive definite and slowly time-varying. To satisfy (30), $\boldsymbol{\Pi}_3$ and $\boldsymbol{\Pi}_4$ should be chosen such that their determinants approach ∞ in addition to the positive definite property. To achieve this, we can select $\boldsymbol{\Pi}_3$ and $\boldsymbol{\Pi}_4$ such that they are diagonal matrices whose main diagonal elements assume very large positive values.

Now integrating both sides of (32) and (33) yields

$$\mathbf{K}_p(t) = \mathbf{K}_p(0) + \alpha_1 \int_0^t (\mathbf{P}_2\mathbf{q}_e + \mathbf{P}_3\dot{\mathbf{q}}_e)\mathbf{q}_e^T dt \tag{34}$$

and

$$\mathbf{K}_d(t) = \mathbf{K}_d(0) + \alpha_2 \int_0^t (\mathbf{P}_2\mathbf{q}_e + \mathbf{P}_3\dot{\mathbf{q}}_e)\dot{\mathbf{q}}_e^T dt \tag{35}$$

where $\mathbf{K}_p(0)$ and $\mathbf{K}_d(0)$ are initial conditions of $\mathbf{K}_p(t)$ and $\mathbf{K}_d(t)$, respectively and can be set arbitrarily.

Solutions for the controller gain matrices of the adaptive controller are given in (34) and (35). The adaptation scheme, as illustrated in Figure 3 is mainly based on the errors of the joint variables of the slave arm and the submatrices of $\mathbf{P}$. Since $\mathbf{P}$ is a constant matrix and $\mathbf{q}_e$ can be easily computed from the desired and actual joint variables available from the master arm system and feedback data, respectively, the computation time required to calculate the adaptive control law given in (2) is relatively small. Consequently, high sampling rates up to 1 KHz can be utilized in the implementation of the proposed control scheme. Thus the manipulator dynamics can be considered *almost constant* during each sampling interval of typically about 1 ms. This feature of the proposed scheme is very attractive to real-time control implementation. We also observe that unlike other conventional adaptive control schemes designed using MRAC, the implementation of the developed adaptive control scheme does not require the slave arm dynamics.

4 COMPUTER SIMULATION STUDY

In this section, using computer simulation we examine the performance of the developed adaptive control scheme which is applied to control the motion of the 7-DOF RRC slave arm illustrated in Figure 4. A complete list of the slave arm parameters can be found in [21]. In the following we will report two study cases. In the first case, the slave arm is controlled so that the 7 joints variables follow a set of desired ramp trajectories while suffering from step change of payload. In the second case, the 7 joint variables are controlled to track a set of desired sinusoidal trajectories during step changes in payload. In the second case, we will also compare the performance of fixed-gain controller versus the developed adaptive controller in terms of tracking capability. The computer simulation study is performed using a modified version of Manipulator Simulation Program (**MSP**) [21].

Controller Parameters

- *Adaptive Controller*: ξ_i and ω_i for i=1,2 were selected so that 2 characteristic roots of (10) are -1 and -2. In this case, we have $\mathbf{D}_1 = 2\mathbf{I}_7$ and $\mathbf{D}_2 = 3\mathbf{I}_7$. Selecting $\mathbf{Q}_i = \mathbf{I}_{14}$ for i=1,2,...,6 and solving (21) using MATLAB we obtain $\mathbf{P}_2 = \mathbf{P}_3 = 0.25\mathbf{I}_7$. The adaptation law can be now implemented by substituting the derived values of $\mathbf{P}_2$ and $\mathbf{P}_3$ into (34)-(35) where $\mathbf{K}_p(0)$ and $\mathbf{K}_d(0)$ can be arbitrarily set. The scalars α_1 and α_2 can be adjusted to improve the tracking quality provided that they always assume positive values.

- *Fixed-Gain Controller*: In the case of fixed-gain controller, we use $\mathbf{K}_p$ = diag(2925, 1912.5, 630, 360, 607.5, 24.4125, 5.67) and $\mathbf{K}_d$ = diag(416, 272, 89.6, 51.2, 86.4, 3.472, 0.8064), which are identical to $\mathbf{K}_p(0)$ and $\mathbf{K}_d(0)$ of the adaptive controller, as specified above.

4.1 Payload Change

Step change in payload occurs when the slave arm drops a load it is carrying, performs some tasks, and picks up the same load later. To study the adaptability of the control schemes in the above situation, we first set the payload at 70 lb. and drop it to 1/3 of the initial payload at 1/3 of the simulation time and then increase it to full payload at 2/3 of the simulation time. Sudden payload changes are modeled by delayed step functions.

4.2 Tracking Ramp Trajectories

In this case the adaptive control scheme is applied to control the motion of the slave arm so that its joint variables follow a set of desired ramp trajectories. For each joint, the initial (**I**) and final (**F**) desired joint angles (**A**) are specified by the user, and the desired velocity is simply obtained by dividing the difference between the final and initial desired joint angles by the simulation time which is 50 seconds in all cases. Initial and final joint angles used in this case are given in the following vectors showing the data in the order starting with Joint 1 and ending with Joint 7: IA = (0, 90, 0, 0, 0, 0, 0); FA = (195, 250, 305, 128, 200, 95.5, 270) with all data in degrees. Simulation results presented in Figure 5 show that the joint angles track their corresponding desired trajectories very closely with some negligible off-track errors in Joints 3, 4 and 6 at the transition of sudden payload changes.

4.3 Tracking Sinusoidal Trajectories

In this case the slave arm is controlled so that its joint angles track a set of desired sinusoidal trajectories. The desired trajectory is specified by $q_i(t)$ = IA + 229sin(Vt) where IA denotes the initial joint angle, V = $\frac{\pi}{t_f}$ and with t_f = 50 seconds, the simulation time. The desired velocity is obtained as $\dot{q}(t)$ = 229Vcos(Vt). In this case we use IA = (0, 30, 60, 0, 30, 60, 90) and from q_i the desired final angle at the end of the simulation is equal to IA. Figure 6 presents the simulation results which show excellent tracking quality in all joints despite sudden change in payloads. Finally, to make a comparative evaluation of the developed adaptive control scheme, we now control the slave arm using the fixed-gain controller as specified before to track the same sinusoidal trajectories as in the case of the adaptive controller. As Figure 7 illustrates, tracking quality is deteriorated in Joints 6 and 7 because the controller is unable to react to the dynamic and static coupling between the joints and to sudden change in payload.

5 CONCLUSION

In this report, employing the concept of model reference adaptive control and Lyapunov method, we have developed a joint-space adaptive control scheme which is suitable for controlling non-compliant motion of robot manipulators performing slowly varying motion. The developed adaptive control scheme was applied to control the motion of the kinematically redundant slave arm of a telerobot system built at Goddard Space Flight Center to study teleoperation. Computer simulation of the control scheme implementation showed that the adaptive control scheme provided good tracking quality in spite of dynamic and static coupling between joints and sudden change in payload. Simulation results also showed that fixed-gain controller failed to effectively react to above disturbances. Current research activities are focusing on the development of an adaptive control scheme in Cartesian space for redundant manipulators and on compliant control of the slave arm motion using a hybrid position/force control [17].

References

[1] JPL, "Telerobotics Project Plan," *Jet Propulsion Laboratory*, JPL D-5692, August 1988.

[2] Kan, E.P., Austin, E., "The JPL Telerobot Teleoperation System," *Robotics and Manufacturing: Recent Trends in Research, Education, and Application*, edited by M. Jamshidi et al, ASME Press, New York, pp. 577-585, 1988.

[3] Schnurr, R., O'brien, M., Cofer, S., "The Goddard Space Flight Center (GSFC) Robotics Technology Testbed," *NASA Conference on Space Telerobotics*, Pasadena, January 1989.

[4] Klein, C.A., Huang, C.H., "Review of Pseudoinverse Control for Use with Kinematically Redundant Manipulators," *IEEE Trans. Sys., Man, and Cyber.*, pp. 245-250, March 1983.

[5] Hanafusa, H., Yoshikawa, T., Nakamura, Y., "Analysis and Control of Articulated Robot Arms with Redundancy," *Proc. 8th IFAC Triennial World Congress*, Kyoto, Japan, pp. 1927-1932, 1981.

[6] Yoshikawa, T., "Analysis and Control of Robot Manipulators with redundancy," *Proc. 1st Intern. Symp. on Robotics Research*, New Hampshire, pp. 735-747, 1983.

[7] Baillieul, J., Hollerbach, J., Brockett, R., "Programming and Control of Kinematically Redundant Manipulators," *Proc. 23rd IEEE Conf. on Decision and Control*, pp. 768-774, 1984.

[8] Luh, J.Y.S., "Conventional Controller Design for Industrial Robots-A Tutorial," *IEEE Trans. Systems, Man, and Cybern.*, Vol. SMC-13, No. 3, pp. 298-316, 1983.

[9] Hsia, T.C., "Adaptive Control of Robot Manipulators: A Review," *Proc. IEEE Conf. on Robotics and Automation*, San Francisco, pp. 183-189, 1986.

[10] Seraji, H., "A New Approach to Adaptive Control of Manipulators,", *ASME Journal of Dynamic Systems, Measurement, and Control*, Vol. 109, pp. 193-202, 1987.

[11] Lim, K.Y., and Eslami, M., "Robust Adaptive Controller Designs For Robot Manipulator Systems," *Proc. IEEE Conf. on Robotics and Automation*, San Francisco, pp. 1209-1215, 1986.

[12] Daneshmend, L.K. and Pak, H.A., "Model Reference Adaptive Control of Feed Force in Turning," *Trans. ASME, Journal of Dynamic Systems, Measurement, and Control*, Vol. 108, pp. 215-222, September, 1986.

[13] Houshangi, N. and Koivo, A.J., "Eigenvalue Assignment and Performance Index Based Force-Position Control with Self-Tuning For Robotic Manipulators," *Proc. IEEE Conf. on Robotics and Automation*, pp. 1386-1391, 1987.

[14] Seraji, H., "Decentralized Adaptive Control of Manipulators: Theory, Simulation, and Experimentation," *IEEE Trans. Robotics and Automation*, Vol. 5, No. 2, pp. 183-201, April 1989.

[15] Nguyen, C.C., Pooran, F.J., "Joint-Space Adaptive Control of Robot End-Effectors Performing Slow and Precise Motions," *Proc. 21st Southeastern Symposium on System Theory*, Florida,pp. 547-552, March 1989.

[16] Nguyen, C.C., Pooran, F.J. "Kinematic Analysis and Workspace Determination of a 6 DOF CKCM Robot End-Effector," *Journal of Mechanical Technology*, Vol. 20, pp. 283-294, 1989.

[17] Nguyen, C.C., Pooran, F.J., "Adaptive Force/Position Control of Robot Manipulators with Closed-Kinematic Chain Mechanism," in *Robotics and Manufacturing: Recent Trends in Research, Education, and Application*, Chapter 4, edited by M. Jamshidi et al, ASME Press, New York, pp. 177-186, 1988.

[18] Nemec, B., Zlajpah, L., Matko, D., "Adaptive Control of Robots Using the Kalman Filter," *Int. Journal of Robotics and Automation*, Vol. 4, No.1, pp. 19-26, 1989.

[19] Nguyen, C.C., Mosier, G.E., "Model Reference Adaptive Control of a Telerobot System," *Proc. ISMM Intern. Symp. Computer Applications in Design, Simulation and Analysis*, Nevada, pp. 282-285, Feb. 1989.

[20] Landau, Y.D., *Adaptive Control: The Model Reference Approach*, Marcell Dekker, New York, 1979.

[21] Chen, J., Ou Y.J., "Dynamic Formulation for Efficient Digital Simulation of Telerobotic Manipulation," *Final Report, Grant No. NAG 5-1019* NASA/GSFC, December 1988.

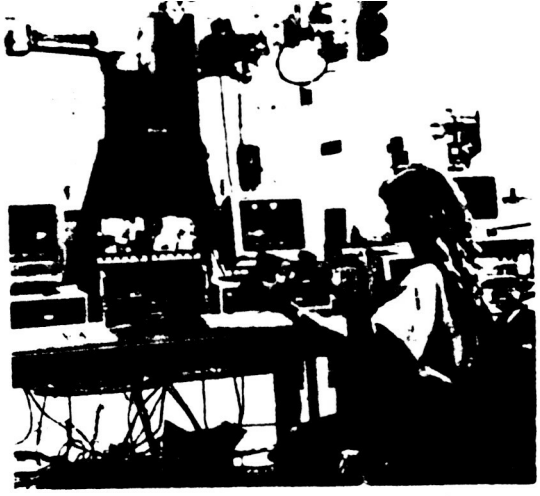

Figure 1: The GSFC Telerobot Testbed

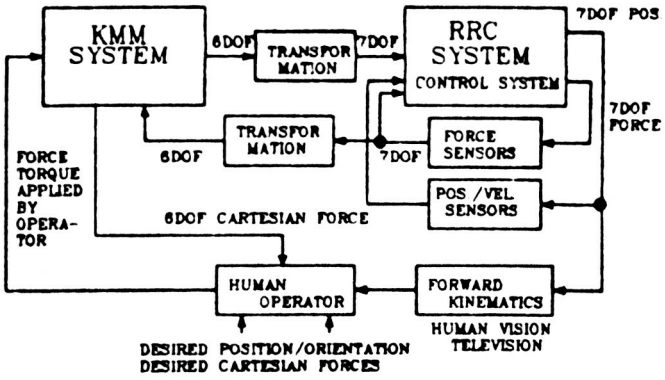

Figure 2: Block Diagram of the Telerobot Testbed

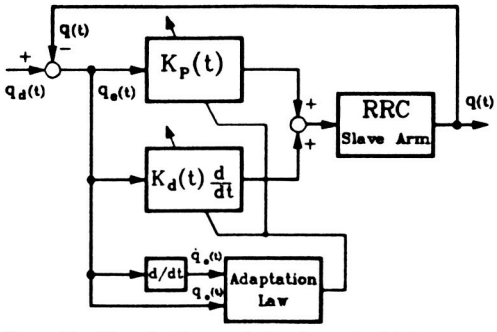

Figure 3: The adaptive control scheme in joint-space

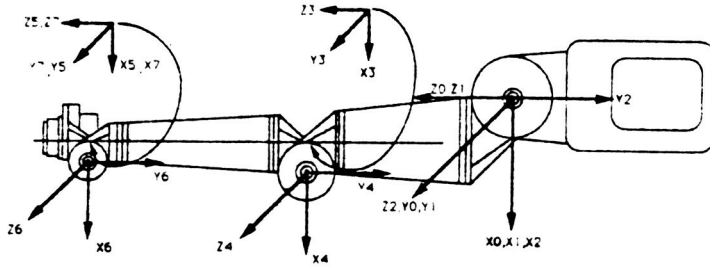

Figure 4: The 7-DOF RRC Slave Arm

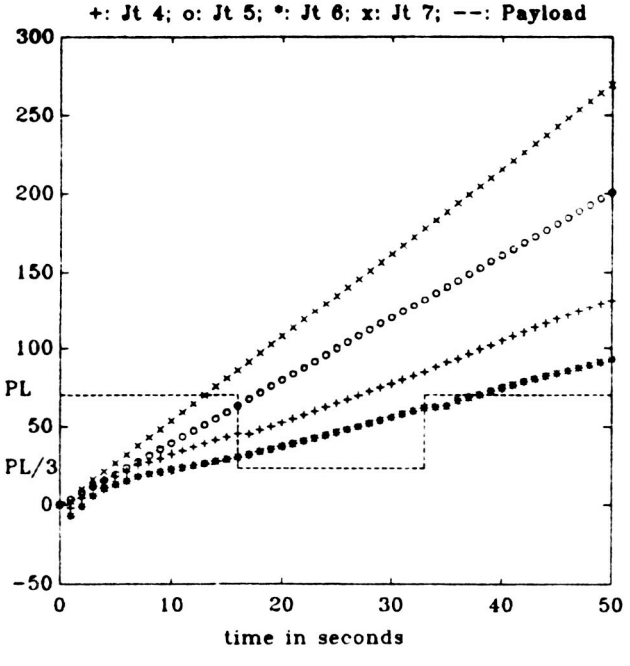

Figure 5a

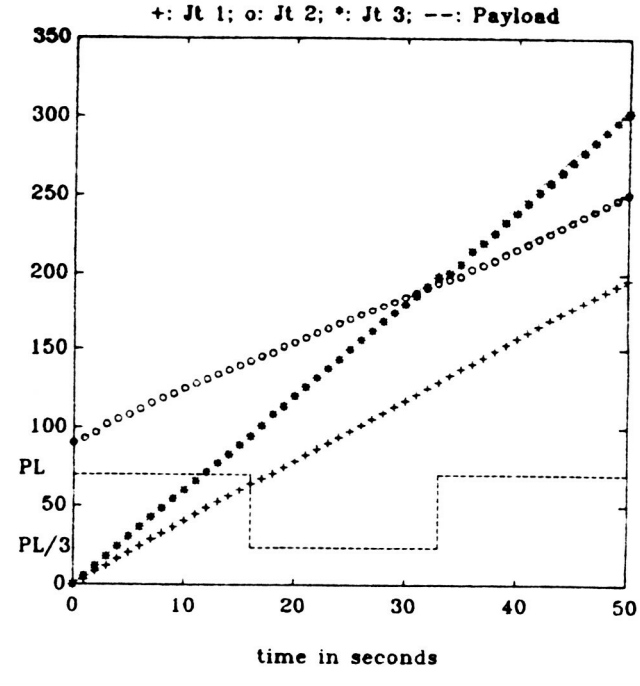

Figure 5b

Figure 5: Tracking Ramp Trajectories

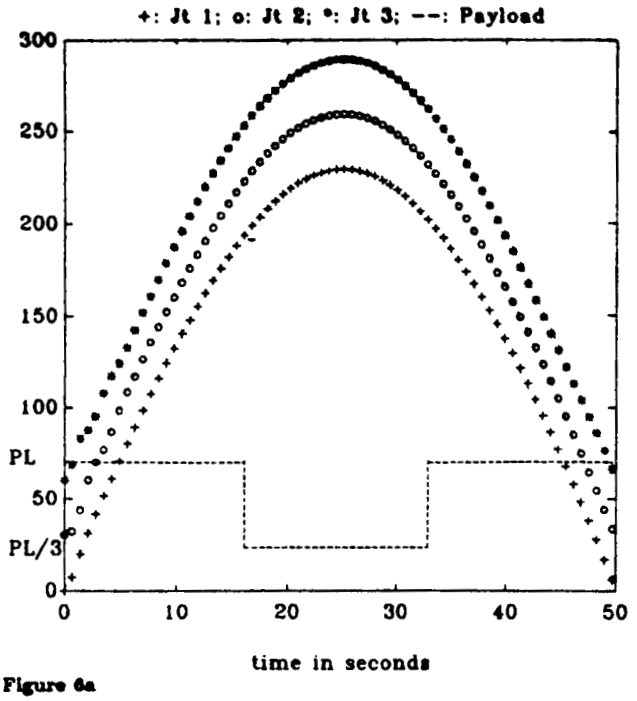

Figure 6a

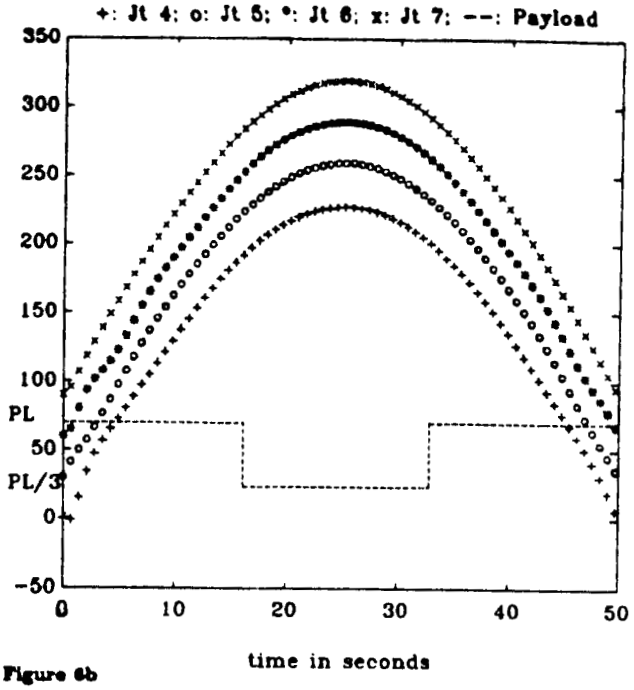

Figure 6b

Figure 6: Tracking Sinusoidal Trajectories

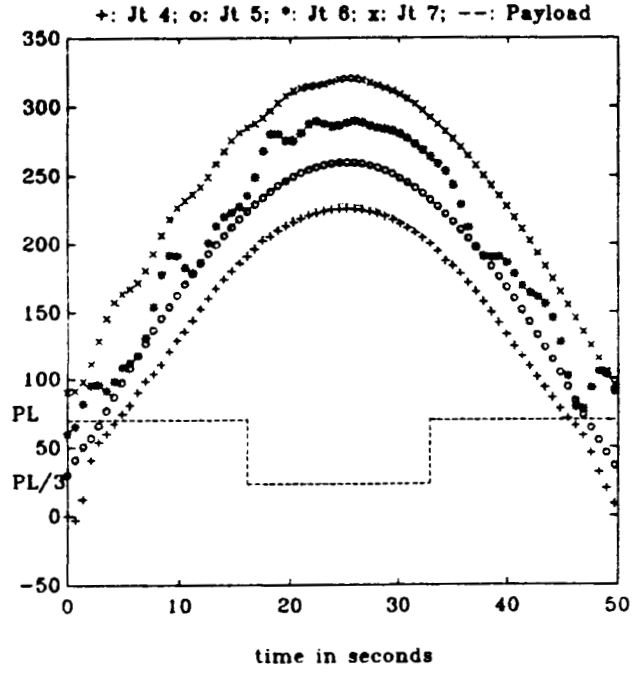

Figure 7a

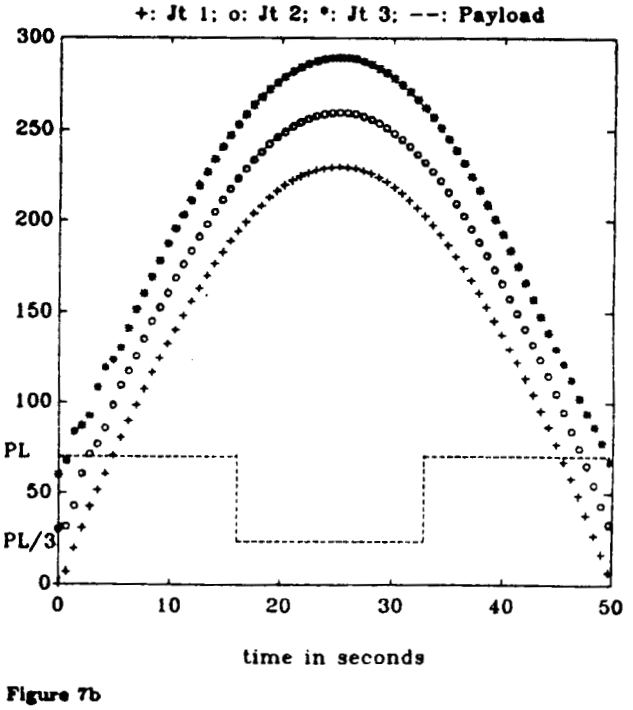

Figure 7b

Figure 7: Tracking using Fixed-Gain Controller